行政院國家科學委員會專題研究計畫 期中進度報告

新的形狀記憶合金之研究--以微力學模擬新的形狀記憶合金特性之研究(2/3)
期中進度報告(精簡版)

計 畫 類 別 ： 整合型
計 畫 編 號 ： NSC 95-2221-E-002-166-
執 行 期 間 ： 95 年 08 月 01 日至 96 年 07 月 31 日
執 行 單 位 ： 國立臺灣大學應用力學研究所

計 畫 主 持 人 ： 舒貽忠

處 理 方 式 ： 期中報告不提供公開查詢

中 華 民 國 96 年 05 月 28 日

行政院國家科學委員會補助專題研究計畫成果報告

新的形狀記憶合金之研究－
以微力學模擬新的形狀記憶合金特性之研究(2/3)

Micromechanics of Novel Shape-Memory Alloys (II)

計畫編號 ： NSC 95-2221-E-002 -166

執行期限 ：95年8月1日至96年7月31日

主持人：舒貽忠副教授　國立台灣大學應用力學研究所

中文摘要

在麻田散鐵材料中所謂的圖案組合指的是如何適當排列麻田散鐵微結構，來降低材料應變能。本文藉由能量最小多重層狀微結構，來提出一套麻田散鐵理論架構，並用來研究在麻田散鐵薄膜變態成為多種兄弟晶微結構的特殊排列方式。該研究指出，麻田散鐵塊材與其薄膜內部所形成之微結構是可以非常不一樣的，薄膜微結構一般具有較簡單之型式。本文預測了非常多在不同方位的麻田散鐵薄膜微結構，所得之結果與 Bhattachary-James 薄膜理論及實驗所觀察到的微結構均相當符合。

註 1：本研究計畫成果報告，預計於近期內投稿至相關學術期刊發表。

註 2：本研究計畫所發展之微結構理論架構，已率先發表於

Y. C. Shu, J. H. Yen, J. Hsieh and J. H. Yeh. “Effect of Depolarization and Coercivity on Actuation Strains due to Domain Switching in Barium Titanate,” *Applied Physics Letters*, Vol. 90, 172902, 2007 (supported by NSC 95-2221-E-002-166).

Pattern Formation in Martensitic Thin Films

Y. C. Shu* and J. H. Yen
Institute of Applied Mechanics, National Taiwan University, Taipei 106, Taiwan, ROC
(Dated: May 28, 2007)

Pattern formation in martensitic materials refers to the accommodation problem of how to mix martensitic variants coherently to minimize the strain energy. A framework based on the ideas of energy minimizing multi-rank laminated microstructure is proposed to study this problem in trigonal martensitic films. It is found that the interfaces between the variants of martensite can be quite different in thin films than in bulk materials and typically have a relatively simple structure. Various intriguing and fascinating self-accommodation patterns are predicted for martensitic thin films with different orientations. The results are in good agreement with the Bhattacharya-James thin-film theory as well as available experimental observations.

Martensitic materials undergo a first-order diffusionless phase transformation during which there is a sudden change in the crystal structure at a certain temperature. Crystals undergoing a thermoelastic martensitic transformation often exhibit the shape-memory effect - a phenomenon where deformation suffered below a critical temperature can be recovered on heating. This unique property has made these alloys used for a variety of applications and attracted as promising candidates for smart materials since they function as actuators as well as sensors [1–3].

A number of recent investigations have suggested that the characteristic distortions of martensite can be exploited to create tiny machines [4]. The key, then, to achieving such an exceptional potential of these materials is to design devices that can take fully advantage of the inherent martensitic microstructure. However, much work has been addressed the problem of pattern formation in martensitic bulk crystals for decades, little has considered it in martensitic thin films except for a variety of experimental examinations. The theoretical study of it has not been proposed until recently by Bhattacharya and James [5] in single crystal films and Shu [6, 7] in polycrystal films. They have found that the interfaces between the variants of martensite can be quite different in thin films than in bulk materials and typically have a relatively simple structure. This prediction enables a novel strategy for the design of micromachines. Examples include tent and tunnel based micropumps obtained by utilizing compatible interfaces between phases to select a unique puzzle with a useful distortion [8]. Such a strategy, on the other hand, requires a detailed understanding of microstructure and its evolution under stress in martensitic films. This in turn calls for a suitable model that can capture the spirit of Bhattacharya-James theory as well as and can be used as a convenient tool to evaluate various conditions in design.

The key feature of a martensitic phase transformation is the microstructure it generates. The high temperature *austenite* phase is cubic while the low temperature *martensite* phase has smaller symmetry. This gives rise to symmetry-related variants which are identical crystal lattices of martensite with different orientations. The transformation from the austenite to the i^{th} variant of martensite is described by the transformation strain $\boldsymbol{\varepsilon}^{(i)}$, and $i = 1 \cdots N$ where N is the number of martensitic variants. It can be determined from the change of symmetry and lattice parameters. In the case of cubic to trigonal transformation, $N = 4$ and

$$\boldsymbol{\varepsilon}^{(1)} = \begin{pmatrix} \alpha & \delta & \delta \\ \delta & \alpha & \delta \\ \delta & \delta & \alpha \end{pmatrix}, \quad \boldsymbol{\varepsilon}^{(3)} = \begin{pmatrix} \alpha & -\delta & \delta \\ -\delta & \alpha & -\delta \\ \delta & -\delta & \alpha \end{pmatrix},$$
$$\boldsymbol{\varepsilon}^{(2)} = \begin{pmatrix} \alpha & -\delta & -\delta \\ -\delta & \alpha & -\delta \\ -\delta & -\delta & \alpha \end{pmatrix}, \quad \boldsymbol{\varepsilon}^{(4)} = \begin{pmatrix} \alpha & \delta & -\delta \\ \delta & \alpha & -\delta \\ -\delta & -\delta & \alpha \end{pmatrix}, \tag{1}$$

where α, δ are material parameters. Let $\boldsymbol{\varepsilon}^*$ be a macroscopically homogeneous strain. It is recoverable if it can be obtained by a coherent mixture of martensitic variants. Indeed, any recoverable strain in this case can be achieved by a rank-3 laminate of variants [9]; i.e.,

$$\boldsymbol{\varepsilon}^* = \sum_{i=1}^{4} \gamma_i \boldsymbol{\varepsilon}^{(i)}, \tag{2}$$

where

$$\begin{aligned} \gamma_1 &= \mu_1, & \gamma_3 &= (1-\mu_1)(1-\mu_2)\mu_3, \\ \gamma_2 &= (1-\mu_1)\mu_2, & \gamma_4 &= (1-\mu_1)(1-\mu_2)(1-\mu_3), \end{aligned} \tag{3}$$

where μ_i is the local volume fraction of some martensitic variants in the i^{th} rank of laminate, and γ_j is the global volume fraction of the j^{th} variant. Notice that $\sum_{i=1}^{N} \gamma_j = 1$. This idea of using an energy minimizing multi-rank laminated microstructure has recently been applied to the study of domain switching in ferroelectric crystals under combined electromechanical loadings (see Fig. 1 therein [10]).

Next, if $\boldsymbol{\varepsilon}^*$ is interpreted as the locally inhomogeneous strain, Eq. (2) still holds if $\gamma_j = \gamma_j(\mathbf{x}) = 1$ if $\mathbf{x} \in \Omega_j$ where Ω_j is the domain occupied by the j^{th} variant of martensite, and $\gamma_j(\mathbf{x}) = 0$ otherwise. These can be achieved if

*Corresponding author. Electronic address: yichung@spring.iam.ntu.edu.tw

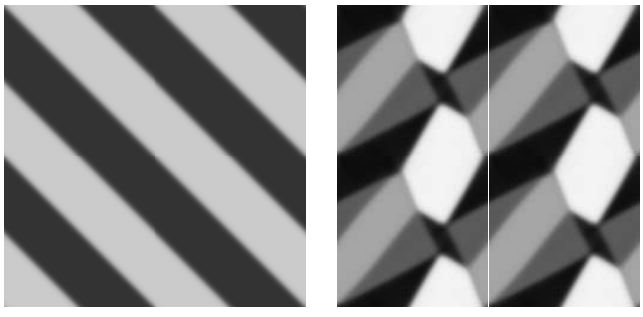

FIG. 1: The LHS and RHS are domain patterns in {100} and {111} films.

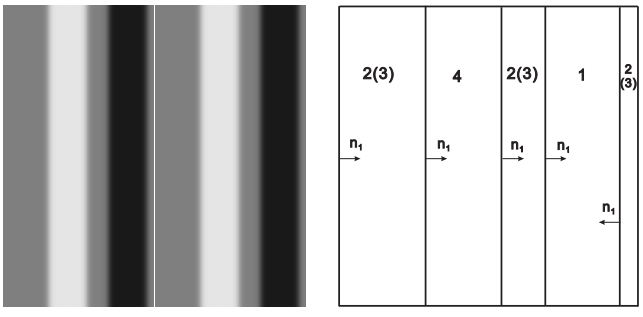

FIG. 3: Another possible domain pattern in {110} films.

{110} Film			
Variants	1, 2 or 1, 3	1, 4	2, 4 or 3, 4
(100) type	(1,0)	(0,1)	(1,0)
(110) type	$(1, \sqrt{2})$	(1,0)	$(-1, \sqrt{2})$

TABLE I: Compatible interfacial normals in a {110} film.

each local volume fraction $\mu_i(\mathbf{x})$ is enforced to be either equal to 0 or 1 at each point $\mathbf{x}$. Thus, when $\gamma_j(\mathbf{x}) = 1$ at some point $\mathbf{x}$, $\gamma_k(\mathbf{x}) = 0$ if $j \neq k$. We now use this idea to study the morphology of martensitic microstructure.

Let $\mu_i(\mathbf{x})$ be relaxed to continuously vary across the sharp interfaces at the boundaries of martensitic variants. The free energy of a martensite at some fixed temperature below the critical temperature is then described in terms of the field variables μ_i by

$$\mathcal{I}(\boldsymbol{\mu}) = \int_\Omega \left\{ W^{int}(\boldsymbol{\mu}) + W^a(\boldsymbol{\mu}) + W^{elas}(\boldsymbol{\mu}) \right\} d\mathbf{x},$$

$$W^{int}(\boldsymbol{\mu}) = A|\nabla \boldsymbol{\mu}|^2, \quad W^a(\boldsymbol{\mu}) = K \sum_{i=1}^{N} \mu_i^2 (1-\mu_i)^2, \quad (4)$$

$$W^{elas}(\boldsymbol{\mu}) = \frac{1}{2} \left[\varepsilon - \varepsilon^*(\boldsymbol{\mu})\right] \cdot \mathbf{C} \left[\varepsilon - \varepsilon^*(\boldsymbol{\mu})\right],$$

subject to the constraint

$$\nabla \cdot \boldsymbol{\sigma} = 0, \quad \boldsymbol{\sigma} = \mathbf{C}\left[\varepsilon - \varepsilon^*(\boldsymbol{\mu})\right], \qquad (5)$$

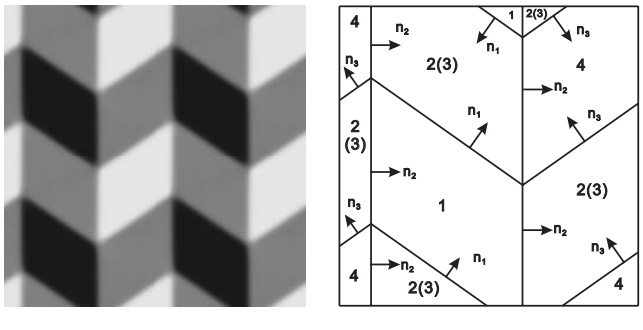

FIG. 2: A domain pattern in {110} films.

where $\boldsymbol{\mu} = (\mu_1, \mu_2, \mu_3)$, and $\mathbf{C}$ is the elastic modulus and is approximated to be same for all phases.

Each of the terms in Eq. (4) has a physical interpretation. The first term, called the *interfacial energy*, penalizes changes in the field, and thus is interpreted as the energy of forming a martensitic interface. The parameter $A > 0$ is related to the length scale of the sharp interface. The second and third terms, W^a & W^{elas}, are the anisotropy and elastic energies. The sum of these two are the energetic cost that the crystal must pay if the field variables and strain deviate from the preferred states; thus this builds in the information that the crystal prefers certain spontaneous strain. The parameter $K > 0$ is related to the strength of anisotropy. Note that the zeros of $(W^a + W^{elas})$ define the the tensorial directions along which the crystal is deformed most easily.

We postulate that the martensitic microstructure is obtained by minimizing the total free energy Eq. (4). However, it is not an easy task. Alternatively, the energy is decreasing if it follows the path

$$\frac{\partial \boldsymbol{\mu}}{\partial t} = -L \frac{\delta \mathcal{I}}{\delta \boldsymbol{\mu}} = L\mathbf{F}, \qquad (6)$$

where $L > 0$ is the mobility, and $\mathbf{F}$ is the *thermodynamic driving force* defined by the variational derivative of the free energy. It is equal to $\mathbf{F}^{int} + \mathbf{F}^a + \mathbf{F}^{elas}$ where $\mathbf{F}^{int} = 2A\nabla^2 \boldsymbol{\mu}$ the driving force due to the formation of interfaces, $\mathbf{F}^a = -\frac{\partial W^a(\mathbf{m})}{\partial \boldsymbol{\mu}}$ the driving force to set each field variable $\boldsymbol{\mu}$ as much close to either 0 or 1 as possible, and $\mathbf{F}^{elas} = \mathbf{C}\left[\varepsilon - \varepsilon^*(\boldsymbol{\mu})\right] \cdot \frac{\partial \boldsymbol{\varepsilon}^*(\boldsymbol{\mu})}{\partial \boldsymbol{\mu}}$ the driving force to align the strain as close on the lowest energy well points as possible.

The present method is similar to the conventional phase field model developed by Khachaturyan, Roytburd, Lookman and their collaborators for martensitic microstructure evolution [11–13]. Their approaches choose a suitable set of order parameters and the specifical polynomial expansions of them at high orders for each specific transformation. Instead, we choose a set of field variables motivated by the hierarchical structure of multi-rank laminates as in Eq. (3). As a result, there is no need to alter the form of the anisotropy energy density

{111} Film						
Variants	1, 2	1,3	1,4	2,3	2,4	3,4
(100) type	$(\sqrt{3},1)$	$(-\sqrt{3},1)$	(0,1)	(0,1)	$(-\sqrt{3},1)$	$(\sqrt{3},1)$
(110) type	$(\sqrt{3},1)$	$(-\sqrt{3},1)$	(0,1)	(1,0)	$(1,\sqrt{3})$	$(1,-\sqrt{3})$

TABLE II: Compatible interfacial normals in a {111} film.

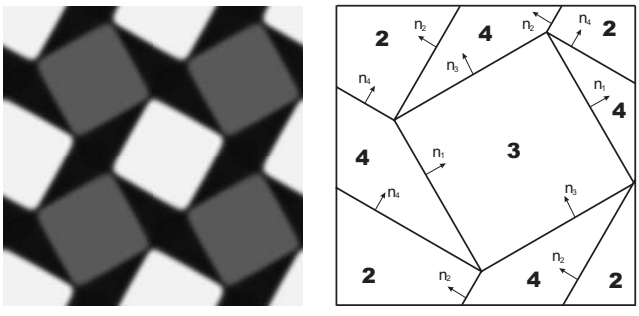

FIG. 4: A domain pattern in {111} film under biaxial tension.

$W^a(\boldsymbol{\mu})$ in Eq. (4) if other martensitic transformations are considered.

We now apply Eq. (6) to study the pattern formation in martensitic thin films undergoing cubic to trigonal transformation at temperature below the critical one. We consider a martensitic single crystal film released from the substrate, but constrained on its lateral boundaries. Suppose the thickness of the film is much smaller than the lateral extent. In this situation, Bhattacharya and James [5] have shown that the out-of-plane of strain incompatibility can be neglected. Therefore, we only need to consider the in-pane components of the transformation strains $\boldsymbol{\varepsilon}^{(i)}$ in Eq. (1). Others such as Eq. (2)-Eq. (6) remain unchanged except that the elastic moduli are replaced by the plane-stress moduli in Eq. (5) and the filed variable $\boldsymbol{\mu} = \boldsymbol{\mu}(x_1, x_2, t)$. Notice that Chen and his collaborators [14, 15] have considered 3D strain compatibility to study domain patterns in tetragonal ferroelectric thin films attached to the substrate.

Depending on the processing techniques and the inherent material properties, the common film normals are {100}, {110} and {111}. Let $\mathbf{R}_{(100)}$, $\mathbf{R}_{(110)}$, and $\mathbf{R}_{(111)}$ be the proper rotations which map $\{100\}\langle 110\rangle$, $\{110\}\langle 110\rangle$, and $\{111\}\langle 110\rangle$ back to the identity. Therefore, the transformation transformations in the reference basis become $\mathbf{R}^T_{(100)}\boldsymbol{\varepsilon}^{(i)}\mathbf{R}_{(100)}$, $\mathbf{R}^T_{(110)}\boldsymbol{\varepsilon}^{(i)}\mathbf{R}_{(110)}$, and $\mathbf{R}^T_{(111)}\boldsymbol{\varepsilon}^{(i)}\mathbf{R}_{(111)}$ for $i = 1, \cdots, 4$. Notice that the thin-film compatibility requires only the in-plane components of the strain to be compatible.

We use Ti-Ni in R-phase as the representative material. This gives $\alpha = 0$ and $\delta = 0.0047$ in Eq. (1) [16]. The elastic moduli of Ti-Ni single crystals are not available, therefore, we take $C_{11} = 80$GPa, $C_{12} = 20$GPa, $C_{22} = 80$GPa, and $C_{13} = C_{23} = 0$ (Voigt notation) which are typical parameters for Ti-Ni polycrystals. The evolution equation in Eq. (6) can be written in the non-dimensionless form. Therefore, the length scale for interfacial boundaries is related to $D = \frac{A/K}{L^2}$ where L is the size of simulation. We take $D = 0.0001$. The constant K is chosen such that W^{elas} to W^a is of the same order. The periodic boundary conditions are taken for simulations and the Fast Fourier Transform is employed to enhance the speed of computation. As the nucleation problem is not considered in the present study, we take the random initial conditions [17].

{100} *films.* In this case, variants 1 & 4 and variants 2 & 3 are indistinguishable since the in-plane components of them coincide. Therefore, there are only two distinct variants and the self-accommodation pattern is the lamellar domain as shown in the LHS of Fig. 1. This pattern is also commonly observed in (100) trigonal film [18].

{110} *films.* In this case, variants 2 & 3 are indistinguishable since the in-plane components of them coincide. Therefore, there are three distinct variants. In a bulk trigonal martensite, there are two typical walls: one is (100) type and the other is (110) type. The corresponding interfacial normals are listed in Table I. The simulation results give two different kinds of self-accommodation patterns as shown in Fig. 2 and Fig. 3. It is interesting to see that Fig. 2 is similar to the commonly observed "herring-bone" type if variants 2 & 3 appear simultaneously in Fig. 2 [1]. Notice that the interfacial normals in Fig. 2 agree well with those listed in Table I. Moreover, another much simpler pattern is shown in Fig. 3. It is not an allowable self-accommodation pattern in bulk martensites since the third components in the interfacial normals are different. However, it is a legitimate pattern in thin films.

{111} *films.* All the in-plane transformation strains are different in this case. As a result, the self-accommodation pattern contains all of the 4 martensitic variants as shown in the RHS of Fig. 1. Moreover, as the shape-memory film is typically stressed under pressure when used as a micropump, we can model it by applying a bi-axial tension in the plane of the film. The simulation result is shown in Fig. 4. Notice that the variant 1 disappear due to the energetic argument. In addition, the final morphology is also a compatible pattern by comparing the RHS of Fig. 4 to Table II.

The authors are glad to acknowledge the financial support of the National Science Council of Taiwan under the grant NSC 95-2221-E-002-166.

[1] K. Otsuka and C. M. Wayman. *Shape Memory Materials.* Cambridge University Press, Cambridge, 1998.

[2] S. K. Wu and H. C. Lin. Recent Development of TiNi-based Shape Memory Alloys in Taiwan. *Materials Chem-*

istry and Physics, **64**:81–92, 2000.

[3] K. Bhattacharya. *Microstructure of Martensite*. Oxford University Press, Oxford, 2003.

[4] K. Bhattacharya and R. D. James. The Material is the Machine. *Science*, 307:53–54, 2005.

[5] K. Bhattacharya and R. D. James. A Theory of Thin Films of Martensitic Materials with Applications to Microactuators. *J. Mech. Phys. Solids*, 47:531–576, 1999.

[6] Y. C. Shu. Heterogeneous Thin Films of Martensitic Materials. *Arch. Rational Mech. Anal.*, **153**:39–90, 2000.

[7] Y. C. Shu. Shape-Memory Micropumps. *Materials Transactions*, **43**:1037–1044, 2002.

[8] K. Bhattacharya, A. DeSimone, K. F. Hane, R. D. James, and C. J. Palmstrøm. Tents and Tunnels on Martensitic Films. *Materials Science and Engineering A*, 273-275:685–689, 1999.

[9] K. Bhattacharya. Comparison of the Geometrically Nonlinear and Linear Theories of Martensitic Transformation. *Cont. Mech. Thermodyn.*, **5**:205–242, 1993.

[10] Y. C. Shu, J. H. Yen, J. Shieh, and J. H. Yeh. Effect of Depolarization and Coercivity on Actuation Strains due to Domain Switching in Barium Titanate. *Applied Physics Letters*, **90**:172902, 2007.

[11] J. Slutsker, A. Artemev, and A. L. Roytburd. Morphological Transition of Elastic Domain Sturctures in Constained Layers. *Journal of Applied Physics*, **91**:9049–9058, 2002.

[12] T. Lookman, S. R. Shenoy, K. Ø. Rasmussen, A. Saxena, and A. R. Bishop. Ferroelastic Dynamics and Strain Compatibility. *Physical Review B*, **67**:024114, 2003.

[13] Y. M. Jin, A. Artemev, and A. G. Khachaturyan. Three-Dimensional Field Model and of Low-Symmetry Martensitic Transformations in Polycrystal: Simulation of ζ_2' Martensite in AuCd Aloys. *Acta Materialia*, **49**:2309–2320, 2001.

[14] Y. L. Li, S. Y. Hu, Z. K. Liu, and L. Q. Chen. Phase-Field Model of Domain Structures in Ferroelectric Thin Films. *Applied Physics Letters*, **78**:3878–3880, 2001.

[15] Y. L. Li, S. Y. Hu, Z. K. Liu, and L. Q. Chen. Effect of Electrical Boundary Conditions on Ferroelectric Domain Structures in Thin Films. *Applied Physics Letters*, **81**:427429, 2002.

[16] S. Miyazaki, S. Kimura, and K. Otsuka. Shape-Memory Effect and Pseudoelasticity Associated with the R-Phase Transition in Ti-50.5 at.% Ni Single Crystals. *Phil. Mag. A*, **57**:467–478, 1988.

[17] K. Ø. Rasmussen, T. Lookman, A. Saxena, A. R. Bishop, R. C. Albers, and S. R. Shenoy. Three-Dimensional Elastic Compatibility and Varieties of Twins in Martensites. *Physical Review Letters*, **87**:055704, 2001.

[18] S. K. Streiffer, C. B. Parker, A. E. Romanov, M. J. Lefevre, L. Zhao, J. S. Speck, W. Pompe, C. M. Foster, and G. R. Bai. Domain Patterns in Epitaxial Rhombohedral Ferroelectric Films. Geometry and Experiments. *Journal of Applied Physics*, **83**:2742–2753, 1998.